Ecological Modelling 250 (2013) 45–57

Contents lists available at SciVerse ScienceDirect

Ecological Modelling

journal homepage: www.elsevier.com/locate/ecolmodel

Development and evaluation of a nutrient cycling extension for the LANDIS-II landscape simulation model

Sarah L. Karam[a,*], Peter J. Weisberg[a], Robert M. Scheller[b], Dale W. Johnson[a], W. Wally Miller[a]

[a] Department of Natural Resources and Environmental Science, University of Nevada, Mail Stop 186, 1000 Valley Road, Reno, NV 89512, USA
[b] Department of Environmental Science and Management, Portland State University, PO Box 751, Portland, OR 97207, USA

ARTICLE INFO

Article history:
Received 2 March 2012
Received in revised form
13 September 2012
Accepted 29 October 2012

Keywords:
Succession
Fire regime
Forest restoration
Soil nitrogen
LANDIS
Nutrient cycling

ABSTRACT

Long-term nutrient cycling dynamics are the result of interactions between forest succession, disturbance, nutrient cycling, and other forest processes. We developed NuCycling-Succession, a simple nutrient cycling and succession extension for the LANDIS-II landscape model of forest dynamics, to examine the interactions between these forest processes in order to develop more realistic predictions of forest response to management practices and global change. NuCycling-Succession models carbon, nitrogen, and phosphorus nutrient fluxes and masses associated with the living biomass, dead biomass, soil organic matter, soil mineral N and P, charcoal, and bedrock nutrient pools. It includes direct effects of disturbance events on nutrient cycling as well as indirect effects mediated through changes in forest composition and structure. NuCycling-Succession represents the continuum of decomposition and associated changes in chemistry using annual cohorts of leaf and fine root litter. This formulation includes the interaction of decomposition dynamics with disturbances that affect the forest floor, such as fire. Evaluation of model results relative to field data and results reported in the literature indicate the model adequately represents nutrient pools and fluxes. We present a case study of the effects of changing fire and biomass harvesting regimes on nutrient cycling in the Lake Tahoe Basin. Model results suggest that fire exclusion has resulted in substantially increased mass of nutrient pools. The NuCycling-Succession extension provides a useful simulation framework for exploring how global change factors (climate change, altered disturbance regimes) may influence nutrient cycling processes and nutrient budgets in forested ecosystems.

1. Introduction

Interactions between forest dynamics, disturbance, and nutrient cycling occur across a range of spatial and temporal scales, leading to complex relationships between them that cannot easily be quantified using empirical studies, which necessarily occur at limited spatial and temporal scales (Oreskes et al., 1994). Alternatively, spatially-explicit simulation modeling of these interactions can be used to understand how succession, disturbance, and nutrient cycling interact. Due to nonlinearities in many forest processes across both time and space, the relationships between forest processes at fine and coarse scales may differ substantially, limiting the ability of model formulations to accurately translate across scales (Rastetter et al., 1992). At small spatial scales (i.e., within a forest stand), individual-tree based gap models simulate establishment, growth, competition, and mortality of individual trees and their interactions with environmental conditions, particularly resource availability, within the stand (Bugmann, 2001). These models can have great mechanistic detail for physiological processes, but have limited spatial extent (generally less than 1 km^2), exclude interactions between patches, and frequently lack spatial locations for individual trees, limiting their ability to include disturbances and other large-scale spatial processes (Bugmann, 2001). Although these models can include detailed, mechanistic plant–soil interactions (Bugmann, 2001), they have limited ability to simulate interactions between disturbance and both forest structure and nutrient cycling.

At large spatial scales, forest simulation models focusing on stand production and growth are frequently used to explore the effects of disturbances and forest management actions on forest productivity and carbon sequestration (e.g., Peng and Apps, 1999; Keane et al., 1996; Scheller et al., 2011). Forests are modeled as stands rather than individual trees in the majority of biogeochemical models derived from CENTURY (Parton et al., 1987, 1988) and Biome-BGC (Running and Hunt, 1993), which facilitates the scaling up of results within a forest type (Rastetter et al., 1992). If stands are modeled as forest types, the effects of differences in species composition and age between stands can be obscured

* Corresponding author. Tel.: +1 775 784 6319; fax: +1 775 784 4583.
E-mail addresses: sarahlkaram@gmail.com (S.L. Karam), pweisberg@cabnr.unr.edu (P.J. Weisberg), rmschell@pdx.edu (R.M. Scheller), dwj@cabnr.unr.edu (D.W. Johnson), wilymalr@cabnr.unr.edu (W.W. Miller).

0304-3800/$ – see front matter © 2012 Elsevier B.V. All rights reserved.
http://dx.doi.org/10.1016/j.ecolmodel.2012.10.016

(Ollinger et al., 2002). For example, differences in species' responses to soil nutrient status may result in a significant effect of disturbance on the nutrient status of some species in that forest type, but not others. However, the relationship between disturbance and nutrient status may be undetectable at the stand level due to successional changes in species composition and the associated changes in plant–soil interactions (Ollinger et al., 2002). Alternatively, forest stands can be modeled using individual species and age classes as in the LANDIS-II landscape model of forest dynamics (He and Mladenoff, 1999; Scheller et al., 2007). This model structure allows interactions of species and age composition with other forest processes, including disturbance and nutrient cycling.

LANDIS-II represents forest stands as collections of age cohorts for each species, reducing computational complexity relative to individual tree models while retaining potential interactions of forest composition and structure with other forest processes (He and Mladenoff, 1999; Scheller et al., 2007). Ecological processes in LANDIS-II are represented in separate extensions that interact with the main model core, allowing the inclusion of ecological processes relevant to the ecosystem and question of interest, including succession, disturbance, and nutrient cycling (Scheller et al., 2007). The model structure allows for interactions and feedbacks between these ecological processes, leading to forest dynamics not anticipated by gap models, which lack spatial interactions and disturbance, and by stand-level models, which lack species-level details. A modified version of CENTURY has been incorporated into LANDIS-II and used to examine the effects of wind, harvesting, and species composition on forest carbon (Scheller et al., 2011). However, the generality of the interactions between disturbance and nutrient cycling, importance of processes related to weather and a monthly native time step, and relatively complex parameterization of this model are not suited for all ecosystems or research questions. As an alternative, we developed NuCycling-Succession, a computationally efficient and parsimonious nutrient cycling extension of carbon, nitrogen, and phosphorus for LANDIS-II that includes a more complete representation of the effects of disturbance on nutrient cycling and reduces both the complexity of parameterization and processes to those necessary for an annual time step. NuCycling-Succession explicitly incorporates interactions between forest succession, fire and harvesting disturbances, and nutrient cycling, allowing for differences between species and age cohorts in their response to nutrient availability and forest disturbances.

Our primary objective is to describe the structure of NuCycling-Succession and demonstrate its utility through an application in the Lake Tahoe Basin, where forest structure and fire regime have been substantially altered since Euro-American settlement. Our modeling scenario examines the effects of changing disturbance regimes, particularly fire exclusion and biomass harvesting for forest management, on nutrient pools at the landscape scale. We evaluate the extension by comparing model results to field data and previous empirical studies and present a sensitivity analysis of model results to key parameters.

2. Model design

We developed NuCycling-Succession to simulate key processes of nutrient cycling and their interactions with forest succession, environmental conditions, and fire and biomass harvesting regimes. The extension interacts with the LANDIS-II Core, base fire (He and Mladenoff, 1999), and biomass harvesting (Gustafson et al., 2000) extensions and uses the general framework of the biomass extension (Scheller and Mladenoff, 2004).

2.1. LANDIS-II forest landscape model

LANDIS-II is a landscape model of forest dynamics, including succession, dispersal, disturbance, and forest management processes (He and Mladenoff, 1999; Scheller et al., 2007). Landscapes are represented as a raster map of individual cells linked through seed dispersal and disturbance. These cells are user-classified into "ecoregions" of homogenous environmental conditions according to their soil characteristics, topography, climate, and other site conditions. Maximum annual production, standing biomass, and establishment probabilities for all species differ between ecoregions. Similarly, the landscape is classified into fire regions of characteristic fire frequency, size, and severity distributions. Within each cell, cohorts of different ages and species establish, grow, compete for resources, and die due to senescence, growth, and disturbance, leading to nondeterministic successional dynamics of species in accordance with their life history traits and the frequency and severity of disturbances. Details of LANDIS-II (He and Mladenoff, 1999; Scheller et al., 2007) and the independent extensions for fire (He and Mladenoff, 1999) and harvest (Gustafson et al., 2000) are available elsewhere.

2.2. NuCycling-Succession extension

The NuCycling-Succession extension simulates key processes of nutrient cycling in relation to landscape-level dynamics of fire, biomass harvesting, and vegetation succession, and calculates associated C, N, and P fluxes between nutrient pools (Fig. 1; see Table 1 for acronym and abbreviation definitions). Modeled structures of nutrient pools at a site vary in complexity: living biomass is modeled by tissue compartments (leaves, wood, fine roots, and coarse roots) for each species-age cohort, dead leaves and fine roots are modeled separately by annual cohorts, and dead wood and coarse roots, soil organic matter (SOM), soil mineral N and P, bedrock, and charcoal are modeled as single pools (Fig. 1). The greater complexity of the living and dead biomass pools represents the greater spatial and temporal heterogeneity in these pools and provides more realistic interactions with disturbance processes. Processes associated with each nutrient pool are described in the sections below. The extension operates on an annual time step, and nutrient cycling processes occur in this order: (1) fire and biomass harvesting events change forest structure, ecosystem nutrients, and nutrient availability and form charcoal; (2) generation of the available nutrient pool through decomposition and other mineralization processes; (3) humification of dead biomass into SOM; (4) resource competition and production of biomass; (5) litterfall and mortality; (6) leaching of mineral N.

2.2.1. Living biomass dynamics

Fluxes of living biomass (B) are a function of establishment (E), annual net primary productivity ($ANPP$), turnover of leaves and fine roots (T), age- and growth-related mortality (M), fire-related mortality (FM), and biomass harvesting-related mortality (HM) for each species i and cohort j:

$$\frac{dB}{dt} = \sum_j \sum_i \left(E_{ij} + ANPP_{ij} - T_{ij} - M_{ij} - FM_{ij} - HM_{ij}\right) \quad (1)$$

E_{ij}, $ANPP_{ij}$, T_{ij}, and M_{ij} are modeled as in Scheller and Mladenoff (2004) with modifications to E_{ij} and $ANPP_{ij}$ resulting from the explicit modeling of nutrient cycling. Nutrient uptake is prioritized by cohort age in decreasing order to emulate asymmetric competition associated with deeper rooting depth and greater fine root mass of older cohorts. Use of translocated nutrients ensures $ANPP_{ij} > 0$, even for young cohorts without access to mineral N and P in the soil. This limits E_{ij} of new species-age cohorts to time steps

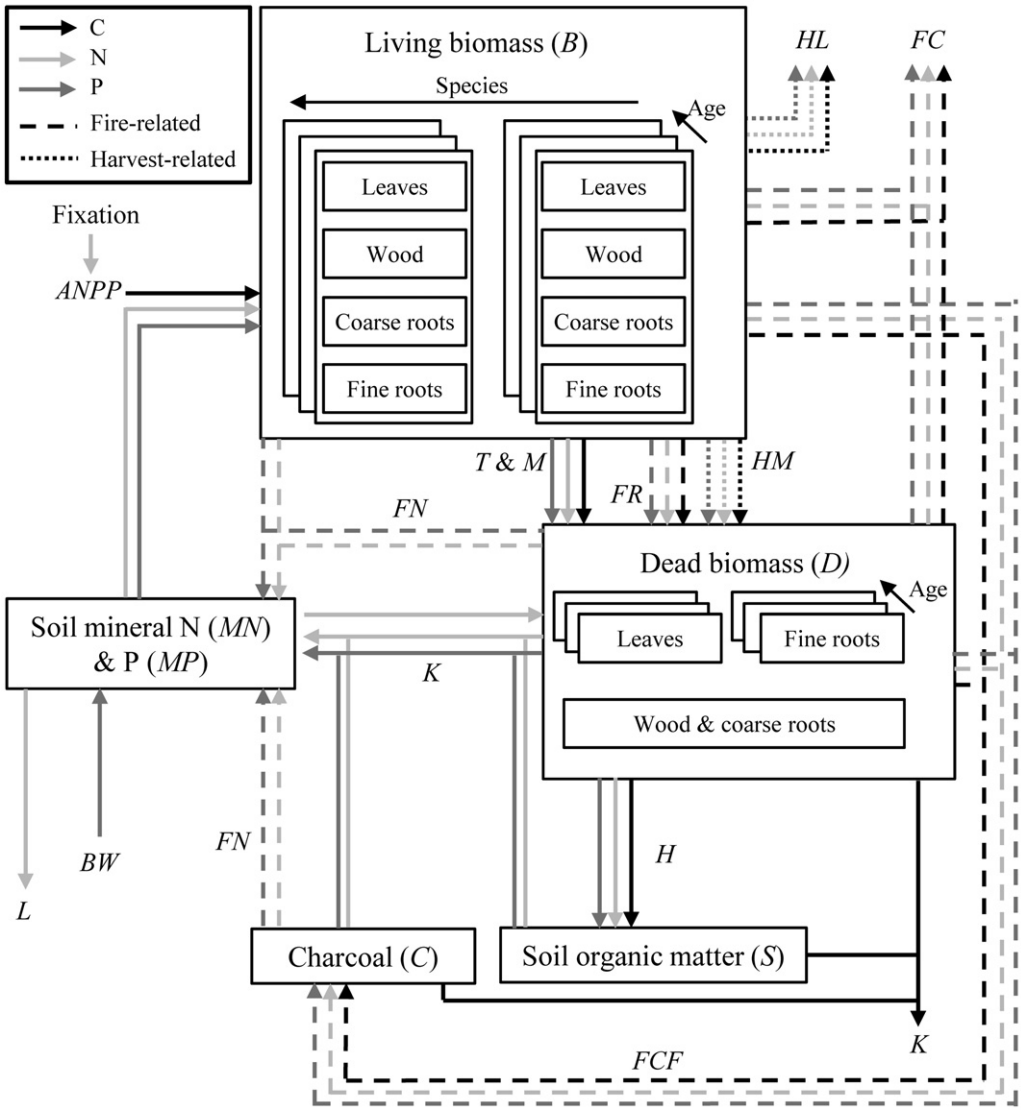

Fig. 1. Modeled C, N, and P fluxes between nutrient pools, including fluxes associated with fire and biomass harvesting events.

when nutrient availability exceeds nutrient uptake by existing vegetation. Mortality (M_{ij}) includes both an age component, which increases exponentially as a cohort approaches its maximum age, and a growth component, which increases according to a logistic function as the actual biomass of a cohort approaches its potential biomass at the site (Scheller and Mladenoff, 2004).

$ANPP_{ij}$ depends on the maximum *ANPP* for the species and available 'growing space', represented as the ratio of current to potential biomass (Scheller and Mladenoff, 2004). Nitrogen, in particular, is a crucial macronutrient and frequently the most limiting nutrient where N deposition is low, fire is frequent, and N-fixing microbial species are relatively rare (Vitousek and Howarth, 1991), so we include a soil N multiplier as a physiological index of plant nutrient status (Pastor and Post, 1985, 1986). The multiplier limits net primary productivity based on the relationship between a species' N tolerance and relative soil N availability as derived from the fertilizer trials of Mitchell and Chandler (1939) and parameterized for a forest gap model by Aber et al. (1979). Species' N tolerances are classified into six levels, with levels 1–3 corresponding to intolerance, intermediate tolerance, and tolerance to low N conditions, and levels 4–6 corresponding to increasing levels of N fixation. Nitrogen fixation contributes to $ANPP_{ij}$ in accordance with the species' N-fixing capability: no N fixation (levels 1–3), low amounts of N fixation (input of up to 30% of required N; generally 20–55 kg N ha^{-1} yr^{-1} for a standing biomass of 25,000 kg), intermediate amounts of N fixation (input of up to 70% of required N; generally 45–100 kg N ha^{-1} yr^{-1} for a standing biomass of 25,000 kg), or high amounts of N fixation (input of 100% of required N; generally 60–140 kg N ha^{-1} yr^{-1} for a standing biomass of 25,000 kg). The amount of N fixed within each range is scaled from zero to the maximum amount according to available soil mineral N, which is preferentially used for species with low and intermediate levels of N fixation, and the biomass of the species relative to its maximum biomass in that ecoregion. Phosphorus limitation of $ANPP_{ij}$ occurs when soil mineral P decreases to zero. N and P translocated prior to T_{ij} and M_{ij} are available for growth the following time step.

E_{ij} and $ANPP_{ij}$ are partitioned into tissue compartments using fixed allometric ratios of 39:61 for deciduous species and 57:43 for evergreen species for aboveground leaf:wood tissues (Niklas and Enquist, 2002), 120:100 for deciduous and 140:100 for evergreen species for fine root:leaf tissues (White et al., 2000), and 22:100 for deciduous and 29:100 for evergreen species for coarse root:aboveground wood tissues (White et al., 2000). Combined, these result in allocation percentages of 24.3% to leaves, 38.1% to wood, 29.2% to fine roots, and 8.4% to coarse roots for deciduous

Table 1
Abbreviations and acronyms.

Notation	Description	Nutrients	Units
AD	Atmospheric deposition	N, P	kg ha^{-1} yr^{-1}
ANPP	Net primary productivity	Mass, C, N, P	kg ha^{-1} yr^{-1}
ANPP^{x}	ANPP exceeding internally available nutrients	N, P	kg ha^{-1} yr^{-1}
B	Living biomass pool	Mass, C, N, P	kg ha^{-1}
BW	Bedrock weathering	P	kg ha^{-1} yr^{-1}
C	Charcoal pool	Mass, C, N, P	kg ha^{-1}
CW	Charcoal weathering	Mass, C, N, P	kg ha^{-1} yr^{-1}
D	Dead biomass pool	Mass, C, N, P	kg ha^{-1}
E	Establishment	Mass, C, N, P	kg ha^{-1} yr^{-1}
FC	Fire-related combustion	Mass, C, N, P	kg ha^{-1} yr^{-1}
FCF	Fire-related charcoal formation	Mass, C, N, P	kg ha^{-1} yr^{-1}
FM	Fire-related mortality	Mass, C, N, P	kg ha^{-1} yr^{-1}
FN	Fire-related mineralization	Mass, C, N, P	kg ha^{-1} yr^{-1}
FR	Fire-related residue moved from *B* to *D*	Mass, C, N, P	kg ha^{-1} yr^{-1}
H	Humification	Mass, C, N, P	kg ha^{-1} yr^{-1}
HL	Harvest-related ecosystem loss	Mass, C, N, P	kg ha^{-1} yr^{-1}
HM	Harvest-related mortality	Mass, C, N, P	kg ha^{-1} yr^{-1}
HR	Harvest-related residue moved from *B* to *D*	Mass, C, N, P	kg ha^{-1} yr^{-1}
i	Species index	–	–
j	Age cohort index	–	–
K	Decomposition	Mass, C, N, P	kg ha^{-1} yr^{-1}
k	Decomposition rate	–	Decimal
L	Leached N	N	kg ha^{-1} yr^{-1}
l	Limit value for decomposition of *D*	–	Decimal
M	Age- and growth-related mortality	Mass, C, N, P	kg ha^{-1} yr^{-1}
MN	Soil mineral N pool (e.g., NH_4^+, NO_3^-)	N	kg ha^{-1}
MP	Soil mineral P pool (e.g., $H_2PO_4^-$, HPO_4^{2-})	P	kg ha^{-1}
[*N*]	Nitrogen concentration	–	Decimal
[*P*]	Phosphorus concentration	–	Decimal
S	Soil organic matter (SOM) pool	Mass, C, N, P	kg ha^{-1}
T	Turnover of leaves and fine roots	Mass, C, N, P	kg ha^{-1} yr^{-1}

species and 29.6%, 22.4%, 41.5%, and 6.5%, respectively, for evergreen species. After accounting for leaf and fine root turnover (T_{ij}), remaining aboveground and belowground mortality (M_{ij}, FM_{ij}, and HM_{ij}) are partitioned proportionally (White et al., 2000), which leads to an increase in the woody proportion of biomass as species-age cohorts mature. Living biomass C, N, and P are calculated from the B_{ij} and static nutrient concentrations for each tissue compartment for each species (Table 2).

Mortality associated with fire (*FM*) and biomass harvesting (*HM*) is partitioned into several fluxes directed toward different nutrient pools. Fire events result in combustion (*FC*), with associated mineralization (*FN*) and charcoal formation (*FCF*), of a portion of the mass and nutrients in aboveground *FM*, leaving the remaining portion as fire residue (*FR*) to be transferred to the dead biomass pool along with the belowground mortality. The proportion of *FM* that is combusted depends on fire severity and the tissue being combusted, with greater *FC* at higher fire severities and for non-woody tissues. *FN* is calculated as a 1% conversion of N and 42% conversion of P in *FC* to mineral forms of N and P, with the difference in rates due to the lower gasification temperature of about 200 °C for N compared to 774 °C for P (Raison et al., 1985). *FCF* is modeled as an 8% conversion of *CM* to charcoal for all nutrients (mean value in Preston and Schmidt, 2006). The remaining C, N, and P in *FC* after accounting for *FN* and *FCF* are volatilized to the atmosphere (Raison et al., 1985). Fire-related E_{ij} and resprouting (contributing to $ANPP_{ij}$) are described in Scheller and Mladenoff (2004).

Biomass harvesting events distribute a portion of aboveground *HM* to ecosystem loss (*HL*) and the remaining portion, along with

Table 2
Selected tissue nutrient concentrations and wood *k* rates for simulated species and functional groups in the Lake Tahoe Basin.

Species or functional group	Live leaf		Dead leaf	Fine root		Wood
	[Lignin]	[N]	[N]	[C]	[N]	*k*
P. jeffreyi/P. ponderosa	0.28	0.009	0.0075	0.49	0.01	0.02
P. lambertiana	0.17	0.009	0.0072	0.48	0.009	0.02
P. contorta	0.1	0.008	0.0062	0.5	0.01	0.02
P. monticola	0.17	0.009	0.0072	0.5	0.016	0.03
P. albicaulis	0.17	0.01	0.008	0.48	0.016	0.03
A. concolor	0.25	0.006	0.0045	0.45	0.01	0.02
A. magnifica	0.31	0.007	0.0054	0.46	0.013	0.02
C. decurrens	0.24	0.007	0.0049	0.48	0.006	0.03
T. mertensiana	0.27	0.007	0.0049	0.5	0.006	0.02
P. tremuloides	0.18	0.008	0.006	0.44	0.0077	0.06
Salicaceae spp.	0.15	0.007	0.0051	0.44	0.0063	0.03
A. incana	0.18	0.008	0.006	0.5	0.008	0.06
A. tridentata	0.16	0.005	0.003	0.49	0.018	0.08
Non-N fixing, resprouting chaparral	0.25	0.008	0.006	0.47	0.0085	0.03
Non-N fixing, obligate seeding chaparral	0.25	0.008	0.006	0.47	0.0082	0.03
N fixing, resprouting chaparral	0.25	0.012	0.011	0.5	0.017	0.06
N fixing, obligate seeding chaparral	0.25	0.01	0.008	0.5	0.016	0.06

all belowground *HM*, to harvest residue (*HR*) that is transferred to the dead biomass pool. These proportions depend on the harvest prescription (Scheller and Mladenoff, 2004).

2.2.2. Dead biomass dynamics

Fluxes of dead biomass (*D*) are modeled separately for leaf, woody, and fine root tissues using differential equations with inputs from turnover (T_{ij}), age- and growth-related mortality (M_{ij}), fire residue (FR_{ij}), and harvest residue (HR_{ij}) for all species-age cohorts. Losses of dead biomass result from decomposition and associated net mineralization (*K*), humification (*H*), and, for aboveground *D*, fire-related combustion (*FC*), and harvest-related loss (*HL*):

$$\frac{dD}{dt} = \sum_j \sum_i (T_{ij} + M_{ij} + FM_{ij} + HR_{ij}) - K - H - FC - HL \quad (2)$$

Influxes of C, N, and P contents for each tissue compartment are calculated as the product of the mass flux and static nutrient concentrations for each tissue compartment for each species. Specifically, nutrient fluxes for T_{ij} and M_{ij} are calculated from nutrient concentrations for tissues after translocation, whereas those for FM_{ij} and HM_{ij} are calculated from nutrient concentrations of living tissues because no nutrients are translocated prior to tissue death. *FC* and *HL* are partitioned in the same manner as those of living biomass as described in section 2.2.1.

K and *H* are modeled with greater complexity for dead leaves and fine roots because of their relative importance to N and P cycling dynamics in comparison to dead woody debris and coarse roots, which contribute less than 5% of mineralized N and 10% of mineralized P (Laiho and Prescott, 2004). In all cases, *K* is a function of *D* and the associated decomposition rate *k*:

$$K = D \times k \quad (3)$$

K and *H* for dead leaves and fine roots are described in Section 2.2.2.1, while those for dead woody debris and coarse roots are described in Section 2.2.2.2.

2.2.2.1. Dead leaves and fine roots. Annual cohorts of dead leaves and fine roots are tracked separately until in a "near-humus" state (Berg, 2000) to emulate the physical stratification of annual forest floor layers. Layers have different physical and chemical properties from neighboring layers due to differences in composition, quantity, and residence time that affect decomposition and mineralization (Berg and McClaugherty, 2010) and the effects of fire (Johnson et al., 1998). Decomposition of dead leaves and fine roots follows the three-phase model outlined in Berg and Staaf (1981) and Berg (2000).

Annual cohorts of dead leaves or fine roots (D_j) are initially comprised of the sum of T_{ij}, M_{ij}, FM_{ij}, and HM_{ij} in that time step, with the associated nutrient contents, decomposition rates (*k*), and limit values to decomposition (*l*) determined using weighted averages based on species composition. Decomposition rates for each species (k_i) are calculated using different empirical models for dead leaves and fine roots. For dead leaves, k_i is a function of the initial lignin and N concentrations of leaves (Table 2) and the actual evapotranspiration (AET) in the ecoregion, a measure of water yield (Eqs. (7), (10), and (11) in Fan et al., 1998). Because root decomposition is relatively insensitive to AET, k_i for dead fine roots is a function of fine root C and N concentrations (Table 2; Fig. 3b in Silver and Miya, 2001). Limit values to decomposition for each species (l_i) define the mass loss at which the remaining material is highly recalcitrant and converted to SOM (Berg et al., 1996). Limit values are calculated from the N concentration of the leaves or fine roots (line 1, Table 6 in Berg et al., 1996).

During Phase One, microbial decomposition (*K*) of an annual cohort D_j can be limited by nutrient supply, so N is immobilized ($K < 0$) from the available mineral pool by the microbial community until a critical C:N ratio of 40 is reached (Prescott et al., 2000). Nitrogen *K* is a function of the C:N ratio of the dead biomass and microbial C:N ratio and C use efficiency (Noij et al., 1993, as formulated in Eq. (4), Verburg and Johnson, 2001) during Phase One. Phase Two marks the beginning of net N mineralization ($K > 0$) proportional to mass loss (Eq. (3)) and is limited by the recalcitrance of the remaining organic material, primarily consisting of lignin and lignified carbohydrates (Berg and Staaf, 1981; Berg, 2000; Moore et al., 2006). During Phases One and Two, carbon *K* exhibits exponential decay (Eq. (3)), and P is conserved ($K = 0$) until the critical C:P ratio of 900 is reached and thereafter mineralized proportionally to mass loss (Prescott et al., 2000; Moore et al., 2006). A critical C:P value of 900 balances the observation that dead materials with higher initial C:P values tend to release P at high critical values (Manzoni et al., 2010) with the observation that litters with initial C:P values less than 700 tend not to retain P (Moore et al., 2006). D_j remains in Phase Two until the limit value *l* is reached, at which point *k* slows and the material is primarily recalcitrant and homogenized (Berg et al., 1996). The remaining material (*H*) is humified and transferred to the SOM pool, in which Phase Three decomposition occurs (Section 2.2.3).

2.2.2.2. Dead wood and coarse roots. Dead wood and coarse roots are combined into a single pool *D* with nutrient contents and the decomposition flux (*K*) determined as a weighted average of *D* and the nutrient contents and k_i of new inputs from T_{ij}, M_{ij}, FM_{ij}, and HM_{ij} that vary by species (Table 2). Dead wood *k* has not been shown to change consistently with site climate (Harmon et al., 2000), so does not vary spatially with AET or another climatic factor as does dead leaf *k*. Exponential decay of *D* (Eq. (3)) results in proportional losses of biomass, C, N, and P, which accurately represents nutrient mineralization dynamics at annual or greater time scales (Laiho and Prescott, 1999).

2.2.3. Soil organic matter dynamics

SOM is modeled as a single pool *S* with inputs from humification (*H*) of dead biomass and outputs from decomposition (*K*):

$$\frac{dS}{dt} = H - K \quad (4)$$

In Phase Three decomposition, *K* for C, N, and P is proportional to mass loss (Eq. (3)) because material previously reached the critical C:N and C:P ratios in Phase Two decomposition. Decomposition rates (*k*) vary by ecoregion to allow for climate and other site effects. We did not include a specific formula for SOM *k* because these effects and the effects of SOM nutrient ratios are uncertain for annual and longer time steps (Fierer et al., 2005; Davidson and Janssens, 2006). Direct effects of fire and biomass harvesting on SOM are relatively minor and difficult to predict (Johnson and Curtis, 2001; Nave et al., 2011), so are not included.

2.2.4. Soil mineral N and P dynamics

The soil mineral N (*MN*) and P (*MP*) pools are comprised of mineral forms of N (e.g., NH_4^+, NO_3^-) and P (e.g., $H_2PO_4^-$, HPO_4^{2-}) available for plant uptake. Inputs to *MN* include net mineralization associated with decomposition of dead biomass and SOM pools (*K*), fire-related mineralization from living biomass, dead biomass, and charcoal pools (*FN*), charcoal weathering (*CW*), and atmospheric deposition (*AD*). Outputs from *MN* include leaching (*L*) and plant uptake:

$$\frac{dMN}{dt} = K + FN + CW + AD - L - \sum_j \sum_i \left\{ [N]_i (E_{ij} + ANPP_{ij}^x) \right\} \quad (5)$$

Plant uptake is a function of the living tissue N concentrations ($[N]_i$) and establishment (E_{ij}) and annual net primary productivity in excess of internally available N from translocation ($ANPP_{ij}^{x}$) for each species-age cohort. L is the larger of a minimum amount (0.1 kg N ha^{-1}) or remaining MN in excess of 50 kg N ha^{-1} (Verburg and Johnson, 2001).

Fluxes of MP are similar to those of MN, with an additional user-defined input from weathering of mineral bedrock (BW) and no L output due to minimal leaching of P in most ecosystems (Djodjic et al., 2004):

$$\frac{dMP}{dt} = K + FN + CW + AD - BW - \sum_{j}\sum_{i}\left\{[P]_i(E_{ij} + ANPP_{ij}^{x})\right\} \quad (6)$$

where $[P]_i$ represents living tissue P concentrations for each species.

2.2.5. Charcoal dynamics

Charcoal (C) is included as a separate pool from SOM because it decomposes substantially more slowly, supports different microbial communities, and influences ecosystem process rates (Pietikainen et al., 2000). Charcoal formation (FCF) from living and dead biomass adds material to the pool, while weathering (CW) and combustion (FC) remove material from the pool:

$$\frac{dC}{dt} = FCF - CW - FC \quad (7)$$

CW is calculated as weathering of C at a rate of 0.02% (half-life = 3465 years, the low-mid range value in Lutzow et al., 2006), and FC is calculated as an 80% combustion of C (Czimczik et al., 2005). FC is proportioned in the manner described in section 2.2.1 for living biomass.

3. Case study

We parameterized NuCycling-Succession and LANDIS-II for the Lake Tahoe Basin, on the border of California and Nevada (Fig. 2). The Lake Tahoe Basin is located in the eastern Sierra Nevada mountains at an elevation range of ca. 1897 at lake level to 3320 m. Precipitation occurs primarily as snow and varies from 500 to 1500 mm yr^{-1}, with greater precipitation to the west of Lake Tahoe and at higher elevations. Soils are generally poor in C and N and have high P in the north and low P elsewhere due to volcanic versus granitic soil parent materials.

The Lake Tahoe Basin has a complex history of natural and anthropogenic disturbance that we used as the framework to explore the effects of disturbance on forest structure and nutrient cycling. The modeling scenario follows the historical trajectory of changes in disturbance, including 900 years under the "natural" fire regime, then fire exclusion beginning concurrently with a 30-year clearcutting prescription mimicking the "Comstock" clearcut that occurred in 1860–1890 to support mining activities in the region (Manley et al., 2000). Modern biomass harvesting for forest management purposes began in the 1980s and is modeled as beginning in model year 1020, 120 years after the onset of fire exclusion. Both biomass harvesting and fire exclusion continue until the end of the model scenario at year 2000. Under the natural fire regime, fire rotation periods varied from 10 to 420 years (Fig. 2), with fire severity increasing with longer fire rotation periods. The fire rotation period increased to 671 years during the fire exclusion period, allowing for rare, high severity fires. The harvest rotation period for forest management was 112 years, with fuel treatments concentrated and more severe at lower elevations along urban areas. The full parameterization process and parameter values are described in Appendix A.

We examined the effects of changing disturbance regimes on forest structure and nutrient pools and fluxes over model time. We

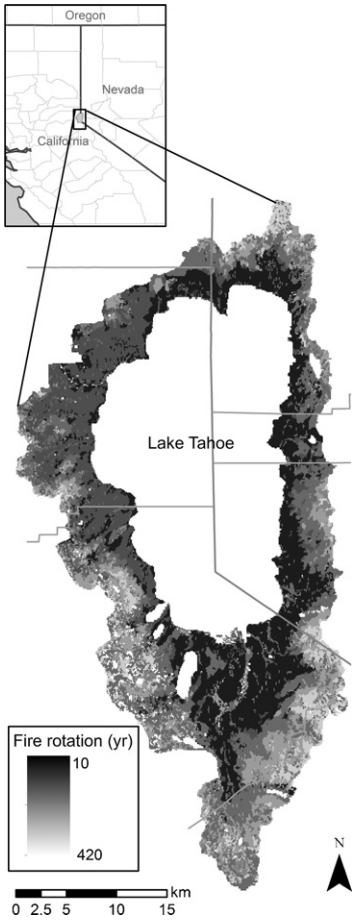

Fig. 2. Simulated fire rotation periods in the Lake Tahoe Basin, showing county lines.

partitioned the change in forest structure and nutrient pools associated with each historical change in disturbance regime (i.e., fire exclusion, the Comstock clearcut, and biomass harvesting for forest management) by running the modeling scenario without each change in disturbance and comparing results to the base scenario, which includes all changes in disturbance regime. We analyzed differences in forest structure and nutrient pools due to each change in the disturbance regime using ANOVA with disturbance change, time step, and their interaction as independent variables (R 2.13.0; R Development Core Team 2011).

3.1. Sensitivity analysis

We evaluated the sensitivity of watershed-level outputs to parameters with limited empirical data in the Lake Tahoe Basin, including the natural fire rotation and severity, total area of the Comstock clearcut, fuel treatment (biomass harvesting) rotation, plant tissue nutrient concentrations (C, N, P, and lignin), and SOM decomposition rates. We also evaluated the sensitivity of several built-in parameters described in section 2.2, including the 1% conversion of N and 42% conversion of P in fire-combusted material (FC) into mineral forms (MN and MP), allometric ratios for biomass partitioning, and critical C:N and C:P ratios indicating the onset of mineralization. For each type of parameter, we repeated one replicate of the model simulation with parameter values ±20%. Output variables included nutrient pools (C, N, and P), forest cover, and biomass by functional group and age category.

We calculated normalized model sensitivity as $I = [(y_2 - y_1)/y_0]/[2\Delta x/x_0]$, where y_0 is the model output calculated with an initial value of x_0 of parameter x and y_1 and y_2

are model outputs calculated with $x_0 \pm \Delta x$ (Lenhart et al., 2002). This yields a dimensionless index for which the sign indicates whether the model output reacts codirectionally (e.g., y increases with an increase in x) or contra-directionally (e.g., y decreases with an increase in x) to the input parameter. We evaluated average sensitivity of each output variable over the entire model run and over the natural fire regime, transition, and treatment time periods associated with changes in fire regimes and fuel treatments. We categorized the index into four classes of sensitivity: negligible ($|I| < 0.05$), medium ($0.05 \leq |I| < 0.20$), high ($0.20 \leq |I| < 1.00$), and very high ($|I| \geq 1.00$) after Lenhart et al. (2002). Very high values indicate that the change in the response variable is more than proportional to the change in the parameter. Sensitivity of the LANDIS-II core model and other extensions has been evaluated elsewhere (Mladenoff and He, 1999; Scheller and Mladenoff, 2004; Wimberly, 2004; Xu et al., 2004, 2005; Scheller et al., 2007; Gustafson et al., 2010).

3.2. Site-level model evaluation

We compared model results for soil and litter concentrations and contents of total C, N, and P at Jeffrey pine- and chaparral-dominated sites to contents of soil and litter samples collected from those vegetation types throughout the Lake Tahoe Basin. For collection of field data, we randomly selected 25 m × 25 m sites of each vegetation type located within two of the lower elevation ecoregions. Samples were collected from 61 Jeffrey pine sites and 52 chaparral sites during summer 2006. At each site, we collected litter and soil samples to 20 cm depth from five points arranged parallel and perpendicular to the down-slope axis at 5 m intervals. We measured litter depth and depth to bedrock at 36 points located every 5 m on a rectangular grid. We dried soil samples at 105 °C and litter samples at 55 °C until at constant weight and determined bulk density. Total C and N concentrations were analyzed using a LECO Truspec® CN analyzer (Leco Corp., St. Joseph, MI) and total P concentrations were determined through ashing at 500 °C, solubilization in 1 N HCl, and vanomolybdenate-blue chemistry (Miller, 1998). We used the mean litter and soil depths to convert concentrations to contents for each site.

To obtain comparable modeled data, we randomly selected nutrient outputs from 61 Jeffrey pine-dominated sites and 52 chaparral-dominated sites in the same ecoregions from model year 1056 (equivalent to the 2006 in the historical trajectory of changing disturbance regimes) that had not experienced fire or harvesting disturbance during the previous 120 simulated years. We used ANOVA with vegetation type and source of data (i.e., field or model) to evaluate differences between actual and modeled values for both soil and litter contents and concentrations.

4. Results

4.1. Case study

Changes in disturbance regimes over time have substantial effects on forest structure and nutrient cycling in the Lake Tahoe Basin. Under the natural fire regime that occurred prior to the onset of fire exclusion, the amount and distribution of biomass among pine, fir, and chaparral functional groups differs in relation to fire rotation period and fire severity (Fig. 3). Frequent, lower severity fire maintains low living biomass (B), with the majority of B in more fire-tolerant species, like pine. For fire regimes with a similar fire rotation period, those with a greater proportion of low severity fire maintain more B.

Relationships between C, N, and P masses of nutrient pools and fire rotation and severity show similar patterns. Because the C, N, and P masses of each nutrient pool are highly correlated ($R^2 \geq 0.90$), we only report values for N. The exception to this pattern is the correlation of soil mineral N (MN) with soil mineral P (MP) ($R^2 = 0.35$), which is lower because ecosystem P loss through volatilization and leaching is substantially lower than ecosystem N loss, so P is retained in the soil in mineral form. Because plant tissue concentrations of P are fixed, constraining uptake, C:N:P ratios of the other nutrient pools remain highly correlated. Nitrogen masses of the B, dead biomass (D), and SOM (S) pools are logarithmically and positively related to fire rotation period ($R^2 = 0.96$, 0.83, and 0.88, respectively) and negatively related to the proportion of fires that are low severity ($R^2 = 0.75$, 0.59, and 0.72, respectively) under the natural fire regime (Fig. 4).

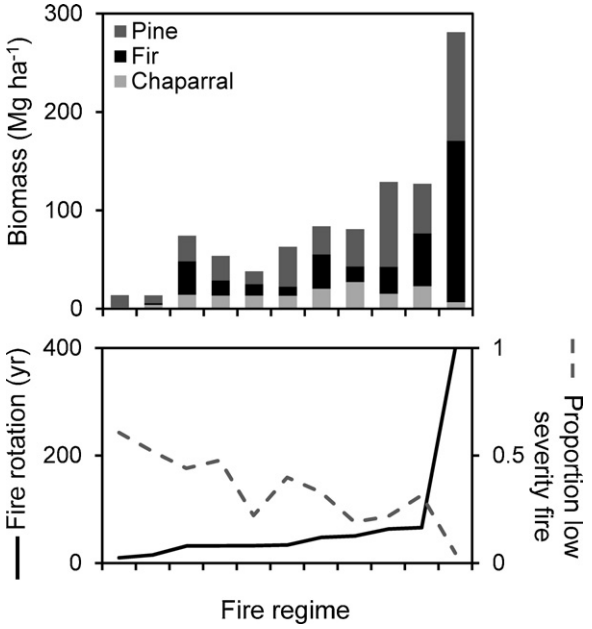

Fig. 3. Biomass of pine, fir, and chaparral functional groups in comparison to fire rotation period and the proportion of fires that are low severity in each natural fire regime.

Changes in disturbance regime lead to a significant shift in forest composition and substantial increases in the masses of B, D, and S nutrient pools (Figs. 5 and 6; Appendix B contains results of the statistical models). Fire exclusion has the largest effect on forest composition and nutrient pools, with omission of the fire exclusion period leading to masses that are significantly lower and similar to those under the natural fire regime (Figs. 5 and 6). Fire reduces aboveground B and D through combustion and volatilization, constraining nutrient availability and productivity and thus biomass and nutrient pool masses. The S nutrient pool experiences a greater proportional change in N mass because longer fire rotation periods allow a greater proportion of annual cohorts of dead leaves to be humified into S, while having no effect on the long residence times of material in the S pool. In our simulation of the Lake Tahoe Basin, this process to humification can require up to 32 years depending on the species, substantially longer than the fire rotation periods across more than 70% of the landscape under the natural fire regime.

The Comstock clearcut and biomass harvesting treatments for forest restoration and fuel reduction have much smaller, though significant, effects on the biomass of functional groups and N mass of nutrient pools. The Comstock clearcut leads to higher B and nutrient pool masses and smaller variability in some of these masses over time than would otherwise occur (Figs. 5 and 6). This is consistent with data from several semi-arid forests showing that

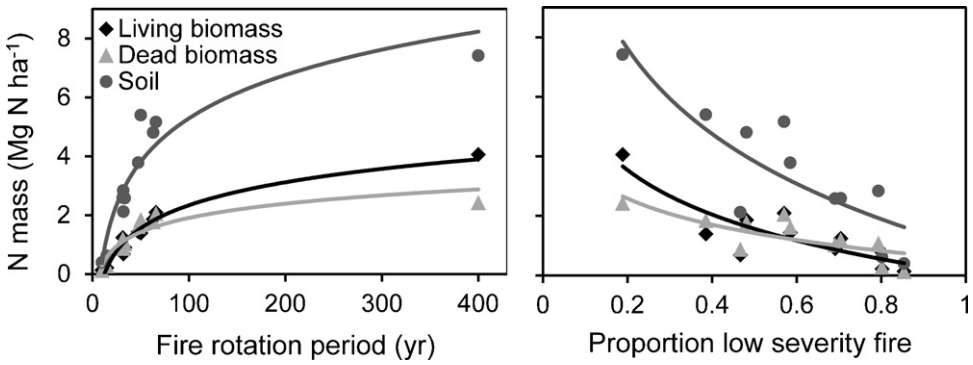

Fig. 4. Scatterplots of mean N masses of nutrient pools as a function of fire rotation period and the proportion of fires that are low severity under the natural fire regimes.

the interaction of fire exclusion and biomass harvesting leads to significantly more homogenous stand structure and higher stand density (Nacify et al., 2010). The biomass harvesting treatments reduce fir biomass per the treatment prescription and have minor effects on nutrient pools because primarily low-nutrient woody material is removed (Figs. 5 and 6). An alternative biomass harvesting prescription, like whole-tree harvesting, would remove more nutrient-rich leaf material, leading to different effects on nutrient cycling.

4.2. Sensitivity analysis

Modeled nutrient pools are more sensitive to changes in parameters than biomass or forest cover outputs (Table 3). Nutrient pools generally exhibit high to very high sensitivities to plant tissue concentrations of the same nutrient (e.g., C pools are highly or very highly sensitive to plant tissue C concentrations) and lower sensitivities to other nutrients (Table 3). Soil organic matter nutrients are highly sensitive to SOM decomposition rates (Table 3), while

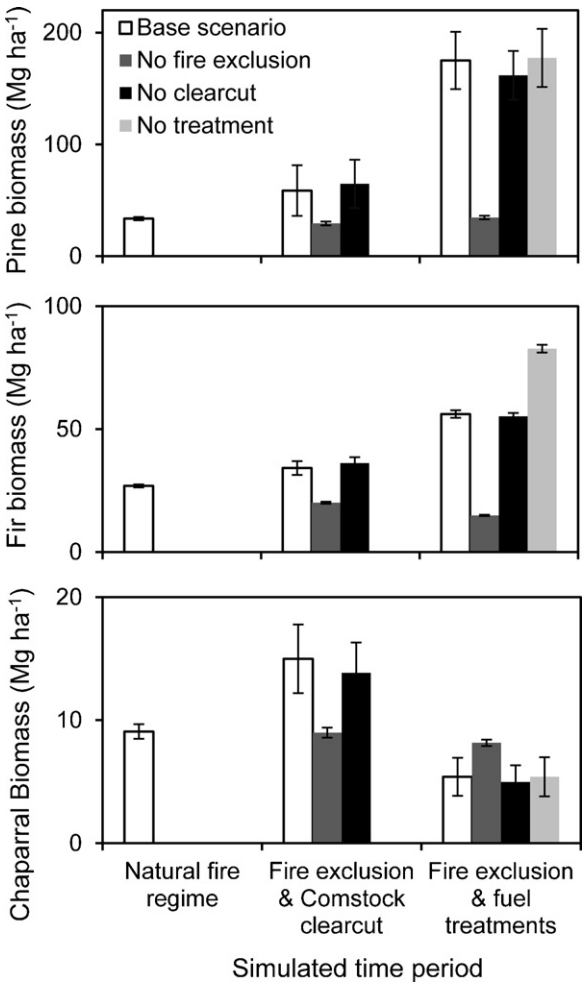

Fig. 5. The mean (±SD) biomass of the pine, fir, and chaparral functional groups under the base scenario compared to scenarios excluding each of the major historical changes in disturbance regime. The three simulated time periods correspond to periods of change in the disturbance regime.

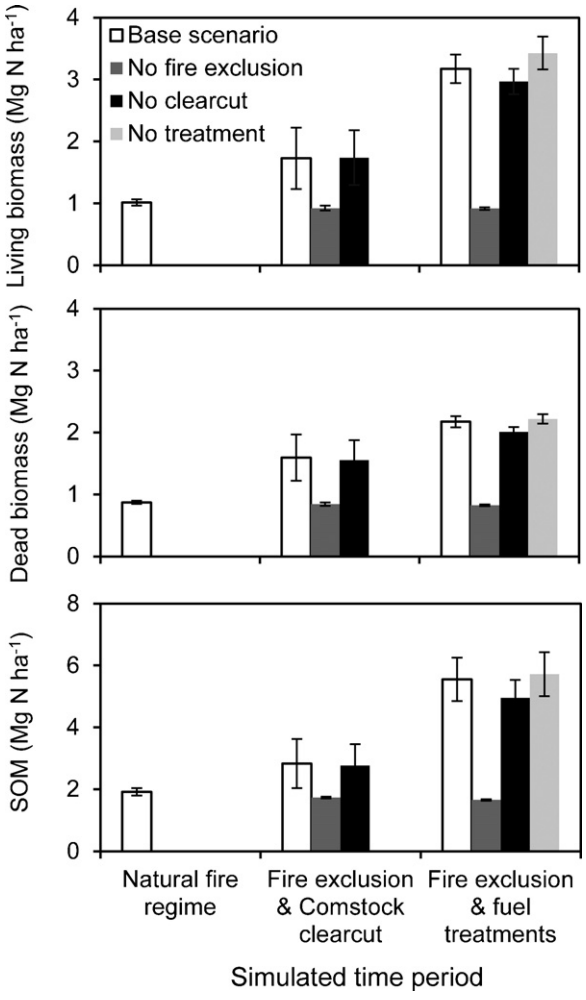

Fig. 6. The mean (±SD) N mass in the major nutrient pools under the base scenario compared to scenarios excluding each of the major historical changes in disturbance regime. The three simulated time periods correspond to periods of change in the disturbance regime.

Table 3
Mean sensitivity index values ($|I| > 0.05$) for the most and least sensitive output variables to user-defined (nutrient concentrations, SOM *k*, fire rotation and severity, and fuel treatment rotation) and built-in (conversion rates of combusted N and P into mineral form, allometric ratios, and critical ratios for mineralization) parameters.

Output	[C]	[N]	[P]	[lignin]	SOM *k*	Fire rot.	Fire sev.	Treat. rot.	Conv. rate	Leaf:wood	Above:below	Critical ratios
Chaparral cover		0.08		0.08	−1[b]	−0.2[b]	3.3[a]	0.3[b]		−0.2[b]	−0.17	−0.08
D (C)	1.1[a]	−0.6[b]		0.3[b]	−1[b]	−0.2[b]	0.3[b]			0.06	−0.16	−0.4[b]
S (C)	1.1[a]	0.2[b]		−0.06	0.14	−0.3[b]	0.3[b]			0.16	−0.07	−0.3[b]
S (N)	1[a]	0.3[b]		−0.09		−0.3[b]	0.3[b]			0.15	−0.05	−1.0[a]
L (N)	−0.17	1.1[a]	−1.1[a]			−0.3[b]	0.9[b]	0.4[b]		0.5[b]	0.4[b]	0.12
Tot[a]l (P)	1.7[a]	0.3[b]	1[b]	−0.08		−0.09	−0.05		−0.19	1.5[a]	1.1[a]	−2.1[a]
D (P)	0.1	−0.8[b]	23.2[a]	0.5[b]		−0.2[b]	0.3[b]	0.07	−1.2[a]	0.9[b]	1.0[a]	−0.9[b]
S (P)	−30.5[a]		1[a]	0.07	−0.7[b]	−0.2[b]	0.7[b]	0.2[b]	−1.5[a]	4.4[a]	4.6[a]	−3.5[b]
C (P)		–	−1.9[a]		−0.07	−0.4[b]	0.7[b]	0.2[b]		0.8[a]	−0.5[b]	−0.14
MP (P)	3.0[a]	0.6[b]		−0.16		−0.15	−0.15		−0.25[b]	1.6[a]	1.1[a]	−4.1[a]
Pine cover						0.09	−0.5[b]	0.05		0.08	0.03	−0.02
Mixed cover	−0.06	0.09			−0.08	−0.08	−0.4[b]			−0.9[b]	−0.8[b]	−0.7[b]
Fir cover	−0.07	−0.16			−0.08	−0.13	−0.11	−0.19		−0.6[b]	−0.5[b]	−0.3[b]
B (tot[a]l)	−0.08	−0.09		−0.07	−0.06	−0.14	−0.17			−1.1[a]	−0.8[b]	−0.6[b]
B (pine)	−0.1	−0.11		−0.1	−0.07	−0.09	−0.5[b]	0.09		−1.6[a]	−1.1[a]	−0.9[b]
B (fir)		−0.3[b]			−0.14	−0.17	−0.12			−1.1[a]	−0.8[b]	−0.6[b]
B (juvenile)	−0.09	−0.3[b]				−0.19	0.06	0.19		−0.5[b]	−0.4[b]	−0.18
B (<25% max age)	−0.1	−0.19		−0.06		−0.2[b]	−0.07	0.2[b]		−0.9[b]	−0.6[b]	−0.4[b]
B (25–50% max age)	−0.06	−0.05		−0.1	−0.09	−0.13	−0.15	0.13		−1.7[a]	−1.2[a]	−1.0[a]
B (50–75% max age)	−0.07			−0.07	−0.05	−0.06	−0.3[b]			−2.1[a]	−1.5[b]	−1.6[a]

[a] $|I| > 1.0$, which signifies a change in the output variable disproportionately larger than the change in the input parameter.
[b] $0.2 < |I| < 1.0$.

other nutrient pools exhibit negligible to medium sensitivities. The P contents of several nutrient pools are highly sensitive to all of the tested built-in parameters (the conversion rate of *FC* into *MP*, allometric ratios, and critical nutrient ratios), while C and N contents are less sensitive (Table 3). Nutrient pool N contents are highly sensitive to the critical C:N ratio, particularly under the natural fire regime when fire is frequent, limiting ecosystem N retention.

Outputs for forest cover class and biomass are most sensitive to allometric ratios, which affect the amount of biomass the plants associated with each forest cover class can produce, and thus the balance of forest cover classes. Secondarily, forest cover classes and biomass are sensitive to the critical nutrient ratios, which regulate nutrient availability for plant uptake. In both cases, chaparral responds codirectionally to changes in allometric ratios because it contains N-fixing species that can maintain productivity with a shift in allocation to N-rich leaf and fine root tissues, while the conifers associated with the other cover classes necessarily reduce their productivity. Of the user-defined parameters, forest cover classes are sensitive to fire severity in relation to the fire tolerance of dominant species in the class and the typical fire regime for the class. Fire-intolerant chaparral, which primarily occurs where fire is frequent, exhibits very high sensitivity. Fire-tolerant pine-dominated and mixed conifer classes, which also occur where fire is frequent, exhibit high sensitivity. The fir-dominated cover class, which consists of species with intermediate fire tolerance and occurs where fire is less frequent, exhibits negligible to medium sensitivity (Table 3). Soil organic matter N and P and leachate N exhibit very high sensitivity to fire severity during the natural fire regime and Comstock clearcut and fire exclusion periods, while other nutrient pools exhibit negligible to medium sensitivity. Model outputs are generally less sensitive to fire rotation than fire severity. All model outputs are negligibly sensitive to clearcut area and treatment rotation. Full results of the sensitivity analysis are available in Appendix C.

4.3. Site-level model evaluation

Modeled values for soil and litter total C, N, and P concentrations and contents in stands dominated by Jeffrey pine and chaparral are not significantly different from those measured in the field (Table 4; $P > 0.05$). Litter C, N, and P contents and soil C and N contents significantly differ between Jeffrey pine and chaparral stands for both modeled values and field measurements ($P < 0.05$); nutrient concentrations of litter and soil do not differ significantly ($P > 0.05$), indicating that differences in litter and soil contents are due to decomposition processes. In general, the variance of modeled contents and concentrations is less than that of the empirical data, likely due to parameterization of the model using the means for all plant nutrient concentrations. Due to the annual temporal resolution and large spatial and temporal scales, we are satisfied with modeling the average condition.

5. Discussion

The NuCycling-Succession extension in LANDIS-II can be used to examine interactions among forest succession, disturbance, and C, N, and P cycling across large temporal and spatial scales. Changes in forest composition and structure are directly linked to nutrient cycling through species' differences in productivity, litter fall and mortality, and dead biomass decomposition rates and limits. The parameterization of ecosystem processes and species characteristics can be altered to reflect changes in disturbance regime (e.g., this study) and climate (e.g., Scheller and Mladenoff, 2005) to examine the effects of these global change factors on nutrient cycling. Results of the case study demonstrate the utility of using NuCycling-Succession and LANDIS-II for understanding large-scale and long-term nutrient cycling dynamics that are difficult to measure empirically. In the Lake Tahoe Basin, the model was used to develop nutrient cycling dynamics under a natural fire regime that no longer exists, providing a measure of the "natural" ("historical") range of variability (Landres et al., 1999) and a baseline for comparison to nutrient cycling dynamics under current and future conditions.

Nutrient pools and fluxes at the 1-ha site scale resulting from the NuCycling-Succession extension generally encompass those observed in empirical studies of nutrient dynamics in the semi-arid western United States (Johnson and Curtis, 2001; Johnson et al., 2007; Boerner et al., 2009). Modeled volatilization fluxes of $-557.68 \pm 9.84\ kg\ N\ ha^{-1}\ yr^{-1}$ compare favorably to empirical estimates based on pre- and post-fire measurements of $-491 \pm 80\ kg\ N\ ha^{-1}\ yr^{-1}$ in mixed conifer forest in the Sierra Nevada mountains (Johnson et al., 2007)

Table 4
Empirical and modeled nutrient concentrations and contents (mean ± SD) in (a) forest floor non-woody dead biomass and (b) soil from Jeffrey pine- and chaparral-dominated stands.

(a) Forest floor		Jeffrey pine		Chaparral	
		Empirical	Modeled	Empirical	Modeled
Concentration (%)	C	50.19 ± 2.53%	50.11 ± 1.08%	50.51 ± 2.27%	50.44 ± 1.10%
	N	0.66 ± 0.13%	0.71 ± 0.10%	0.80 ± 0.28%	0.91 ± 0.16%
	P	0.010 ± 0.002%	0.011 ± 0.003%	0.008 ± 0.005%	0.010 ± 0.004%
Content (kg ha^{-1})	C	14,325 ± 3995.5	11,114 ± 2809.8	22,000 ± 9899.5	14,416 ± 5175.6
	N	285.4 ± 124.9	190.0 ± 138.1	884.0 ± 681.4	407.5 ± 288.1
	P	11.6 ± 3.0	3.8 ± 2.0	21.3 ± 9.0	13.7 ± 6.8
(b) Soil		Jeffrey pine		Chaparral	
		Empirical	Modeled	Empirical	Modeled
Concentration (%)	C	3.33 ± 2.31%	2.08 ± 1.74%	2.73 ± 1.37%	3.04 ± 1.36%
	N	0.09 ± 0.06%	0.05 ± 0.04%	0.09 ± 0.04%	0.12 ± 0.06%
	P	0.009 ± 0.008%	0.015 ± 0.010%	0.018 ± 0.030%	0.014 ± 0.005%
Content (kg ha^{-1})	C	51,228 ± 20,135	43,367 ± 16,119	47,250 ± 19,445	45,367 ± 19,090
	N	2040 ± 507.1	1621 ± 447.1	4043 ± 5394	2918 ± 2744
	P	840.9 ± 414.6	467.3 ± 246.6	531.1 ± 208.8	448.7 ± 138.9

and -653 ± 187 kg N ha^{-1} yr^{-1} from dead biomass and soil pools in more productive mixed conifer forest in central Oregon (Bormann et al., 2008). Similarly, modeled N fixation rates of 19.07 ± 0.08 kg N ha^{-1} yr^{-1} for chaparral with low N-fixing capabilities (e.g., *Ceanothus cordulatus*, *Purshia tridentata*) and 40.60 ± 0.24 kg N ha^{-1} yr^{-1} for chaparral with intermediate N-fixing capabilities (e.g., *C. velutina*) are comparable to a 500–570 kg N ha^{-1} increase in total soil N over 12 years by *C. velutina* in central Oregon (Binkley et al., 1982). Unlike these chaparral species, the riparian species *Alnus incana* has high N-fixing capabilities and will continue to fix N even in N saturated conditions. Its modeled N fixation of 141.43 ± 2.21 kg N ha^{-1} yr^{-1} is within the measured range of 43–360 kg N ha^{-1} yr^{-1} (Haeussler and Coates, 1986).

Modeled N leaching is dependent on site AET, the presence of N-fixing species, and recent fire events. In low elevation mixed conifer forests without fire in the past 5 years, modeled leaching of -0.48 ± 0.03 kg N ha^{-1} yr^{-1} is comparable to empirical estimates of -0.4 ± 0.1 kg N ha^{-1} yr^{-1} at a mixed conifer site in the Lake Tahoe Basin (Murphy et al., 2006; Johnson et al., 2007). Across the entire basin, the mean modeled leaching flux of -3.16 ± 1.14 kg N ha^{-1} yr^{-1} is substantially higher, but incorporates areas of higher precipitation and AET, and so higher leaching potential, and greater biomass of N-fixing species associated with higher elevations and riparian areas. Considering that 96.6% of sites exhibit the minimal leaching rate of -0.1 kg N ha^{-1} yr^{-1}, this higher rate of leaching is clearly driven by a subset of sites. Of the 2.4% of sites with leaching between -10 and -540 kg N ha^{-1} yr^{-1}, 70.2% had experienced fire events in the past 5 years and 21.0% had *A. incana*, a riparian species that can fix excessive amounts of N. Fire can lead to a short term increase in leaching due to an increase in available mineral nutrients in the soil (Murphy et al., 2006; Johnson et al., 2007). Leaching at a mixed conifer site in the Lake Tahoe Basin reached -9.6 ± 3.8 kg N ha^{-1} yr^{-1} after wildfire (Murphy et al., 2006; Johnson et al., 2007), comparable to modeled estimates of -13.1 ± 0.2 kg N ha^{-1} yr^{-1} in the first five years after a wildfire. Whereas both volatilization and N fixation fluxes are directly linked to a spatial location, leaching fluxes may result in an efflux of N from one point and an influx at another point where it is taken up by plants or otherwise immobilized, resulting in a smaller net leaching flux out of the terrestrial ecosystem than location-based results would suggest. Because NuCycling-Succession does not simulate water or its movement, it is unable to account for this potential N sink, and thus may overestimate N leaching.

Although our modeling results are comparable to empirical estimates for soil C and N (Table 4) and N fluxes, a full validation is not possible given the large spatial and temporal scales and historical dependency of our projections. Considering the general comparability of the magnitude of key N fluxes to empirical estimates, we have some confidence in the modeled long-term changes in N cycling dynamics associated with fire and biomass harvesting at the site scale. Like other nutrient cycling models, NuCycling-Succession is expected to have higher heuristic value and lower predictive value due to considerable assumptions about nutrient cycling processes and their interactions (Rastetter, 1996). The addition of more processes, including dynamic spatial movement of ground and surface water, and thus leached nutrients, and aerial transport of ash, an important vector of nutrient movement after fire, may improve model realism, albeit with increased complexity and parameterization requirements.

The NuCycling-Succession extension differs substantially from Fire-BGC (Keane et al., 1996), a landscape model based on Biome-BGC (Running and Hunt, 1993) and the CENTURY model (Parton et al., 1987, 1988), which has been incorporated into LANDIS-II in a modified form (Scheller et al., 2011). Differences in the native spatial and temporal scales, complexity of simulated ecological processes and parameterization, and structure of nutrient pools in each model (Table 5) indicate that each may be particularly well-suited for certain ecosystems and questions. We designed NuCycling-Succession to be a parsimonious model of long-term nutrient cycling dynamics that emphasizes the role of disturbance.

Both CENTURY and Biome-BGC were developed to include water balance as an important driver of nutrient cycling, necessitating a daily or monthly time step and a detailed set of weather-related parameters. These models are well-suited for analysis of the short-term effects of individual disturbance events or changes in weather associated with climate change, but the complexity of parameterization and computation is less suited for examining changes in nutrient cycling at century or longer time scales. In contrast, NuCycling-Succession was developed for an annual time step and incorporates the effects of differences in mean water balance between ecoregions through differences in site productivity and decomposition rates.

Because NuCycling-Succession was designed for the landscape scale, it also includes more detailed interactions between fire and nutrient cycling, including combustion and volatilization, mineralization, and charcoal formation processes with rates that vary based on fire severity and forest composition and structure within each

Table 5
Comparison of model structure and processes in NuCycling-Succession, CENTURY (Parton et al., 1987, 1988), and Fire-BGC (Keane et al., 1996).

	NuCycling-Succession	CENTURY	FIRE-BGC
Modeled nutrients	C, N, P	C, N, P, S	C, N
Native time step	Annual	Monthly	Daily and annual
Spatial scale of nutrient cycling	Raster cell	Raster cell	Simulation plot within a stand
Complexity of effects on nutrient cycling of:			
Water balance	Low	High	High
Fire	High	Intermediate	Low
Harvesting	High	Intermediate	N/A
Nutrient pool structure:			
Living biomass	By species-age cohort	Single[a]	Trees Undergrowth
Dead biomass	Annual cohorts of leaves	Structural residue of leaves Metabolic residue of leaves	Litter and duff
Soil	Annual cohorts of fine roots	Structural residue of fine roots Metabolic residue of fine roots	
	Wood and coarse roots	Wood Coarse roots	Wood
Soil	Mineral nutrients Soil organic matter	Mineral nutrients Fast soil organic matter Slow soil organic matter Passive soil organic matter	Mineral nutrient
	Charcoal		
Complexity of:			
Successional processes	High	Low[a]	Intermediate
Disturbance processes	High	Low[a]	Intermediate

[a] The Scheller et al. (2011) implementation of CENTURY within LANDIS-II is equivalent to NuCycling-Succession.

raster cell. Neither CENTURY nor Fire-BGC includes a charcoal pool or related processes nor, in most applications, do they account for variation in the rates of fire processes. In Fire-BGC, fires occur at the landscape scale, creating stands of homogenous succession stage and disturbance conditions, and nutrient cycling occurs in a simulation plot within the stand. This difference in organization scale prevents variation in the effects of fire on nutrient cycling within a stand and excludes legacy effects of previous forest structure and disturbance, which may lead to unrealistic dynamics. Considering the importance of fire to nutrient cycling in the Lake Tahoe Basin (Figs. 4 and 6) and many other semi-arid forests, the more explicit treatment of fire in NuCycling-Succession may be advantageous in these ecosystems.

The models also differ with regard to nutrient pool structure, with Fire-BGC having the most simple representation and CENTURY and NuCycling-Succession having more complex representations with different emphases. While CENTURY focuses on the dynamics of soil pools and the importance of decomposition to nutrient availability, NuCycling-Succession focuses on living and dead biomass pools and the importance of disturbance. The simple representation of living biomass pools in Fire-BGC and most CENTURY models does not allow for variation in nutrient contents and allocations based on species composition or age distributions, unlike the NuCycling-Succession and CENTURY (Scheller et al., 2011) extensions for LANDIS-II. Both CENTURY and Biome-BGC *a priori* partition non-woody dead biomass and SOM pools into distinct components with different decomposition rates. In contrast, NuCycling-Succession represents cohorts of decomposing material from fine dead biomass to SOM, similar to the continuum model of Berg (2000). In this model, the non-recalcitrant (i.e., metabolic) materials in age cohorts of non-woody dead biomass decompose before the recalcitrant (i.e., structural) materials. When these age cohorts reach a limit value for decomposition, the material is transferred to the single SOM pool (Berg et al., 1996). The cohort model emulates the physical and chemical stratification of annual layers of non-woody dead biomass, allowing decomposition and net mineralization to vary between annual cohorts and within each cohort over time. Thus, an annual cohort in the first decomposition phase may have a net uptake of mineral N while a cohort in the second phase has a net release of mineral N. Until these annual cohorts undergo humification and are transferred to the SOM pool, they are affected by disturbances that affect dead biomass pools, like fire and biomass harvesting. Unlike the discretized pools of dead biomass in Biome-BGC and CENTURY, the cohort model precludes transfer of material to the SOM pool before the limit value for decomposition is reached and the effects of disturbance are realized.

In addition to uncertainty associated with model structure and formulation, there is uncertainty associated with model parameterization. We attempted to quantify this uncertainty with a sensitivity analysis of several user-defined and built-in parameters with limited empirical data or high variability using data for the Lake Tahoe Basin. Although nutrient pools were generally sensitive to nutrient concentrations of plant tissues, which primarily affect the mass of nutrient pools, and SOM decomposition rates, which drive the magnitude of nutrient cycling fluxes, continued empirical research is likely to reduce uncertainty in these parameters. Similarly, the high sensitivity of biomass to built-in allometric ratios (leaf:wood tissues and aboveground:below ground tissues), primarily due to variation in nutrient ratios between different plant tissues, and critical nutrient ratios, which regulate available N and P, is associated with reducible uncertainty. In contrast, uncertainty associated with the attributes of the natural fire regime and biomass harvesting is unlikely to be significantly reduced. Forest cover, biomass, and some nutrient pools are highly sensitive to fire severity under the natural fire regime. A change in fire severity primarily affects the balance between pine and chaparral, with an increasing fire severity associated with a greater shift toward chaparral cover and biomass (Table 3). Although this balance is highly sensitive to fire severity, it is unlikely to change the qualitative dominance of pine. Similarly, N and P masses of some nutrient pools are moderately sensitive to fire severity, but the relative masses of the pools means that the only substantial trade-off is between greater nutrient storage in living biomass under higher fire severities versus greater storage in dead biomass and SOM pools under lower fire severities. Because the combined mass of the dead biomass and SOM pools is over twice the mass of the living biomass pool, even large changes in fire severity are unlikely to change these relationships. Although these uncertainties may reduce our ability

to accurately quantify nutrient pools and fluxes in relation to historical changes in fire and biomass harvesting regimes, the modeling simulation is able to highlight the relative influence of disturbance on nutrient cycling dynamics.

6. Conclusions

Simulation modeling is a powerful tool to examine interactions between succession, disturbances, nutrient cycling, and other ecosystem processes constrained by environmental conditions across large spatial and temporal scales. The NuCycling-Succession extension for LANDIS-II incorporates the effects of fire and biomass harvesting disturbances on nutrient cycling, both directly and as mediated through changes in forest composition and structure. NuCycling-Succession represents decomposition and associated changes in the chemical composition of organic soils of a series of cohorts of decomposing materials. In this formulation, disturbances that affect dead biomass pools, like fire, affect these materials until they are humified into the SOM pool. Assessing the interactive effects of changing climate and disturbance regimes on forest productivity, carbon sequestration, and other ecosystem functions is essential to effective forest management considering accelerated rates of global change.

Model results suggest that changes in disturbance regimes since Euro-American settlement have significantly changed both forest structure and nutrient dynamics in the Lake Tahoe Basin. Fire exclusion appears to have a significantly larger effect on forest structure and nutrient pools than either intense biomass harvesting of short duration (e.g., the Comstock clearcut) or moderate biomass harvesting of a longer duration (e.g., forest management treatments). Considering the prevalence of fire exclusion policies, many forests are likely to have experienced an increase in the mass of nutrient pools.

Acknowledgements

Research was funded by the U.S. Forest Service, Lake Tahoe Basin Management Unit, grant 05-CR-11051900-012. Soils analyses were conducted with Robert Blank and Tye Morgan at the Soil Chemistry Laboratory, Nevada Agricultural Research Station, Reno, NV. We thank two anonymous reviewers for their comments.

Appendix A. Supplementary data

Supplementary data associated with this article can be found, in the online version, at http://dx.doi.org/10.1016/j.ecolmodel.2012.10.016.

References

Aber, J.D., Botkin, D.B., Melillo, J.M., 1979. Predicting the effects of different harvesting regimes on productivity and yield in the northern hardwoods. Canadian Journal of Forest Research 9, 10–14.
Berg, B., Staaf, H., 1981. Leaching accumulation and release of nitrogen in decomposing forest litter. Ecological Bulletins (Stockholm) 33, 163–178.
Berg, B., Ekbohm, G., Johansson, M.-B., Mcclaugherty, C., Rutigliano, F., Virzo De Santo, A., 1996. Maximum decomposition limits of forest litter types: a synthesis. Canadian Journal of Botany 74, 659–672.
Berg, B., 2000. Litter decomposition and organic matter turnover in northern forest soils. Forest Ecology and Management 133, 13–22.
Berg, B., McClaugherty, C., 2010. Changes in substrate composition during decomposition. In: Berg, B., McClaugherty, C. (Eds.), Plant Litter: Decomposition, Humus Formation, Carbon Sequestration. Springer-Verlag, Berlin-Heidelberg, pp. 85–114.
Binkley, D., Cromack Jr., K, Fredriksen, R.L., 1982. Nitrogen accretion and availability in some snowbrush ecosystems. Forest Science 28, 720–724.
Boerner, R.E.J., Huang, J., Hart, S.C., 2009. Impacts of fire and fire surrogate treatments on forest soil properties: a meta-analytical approach. Ecological Applications 19, 338–358.
Bormann, B.T., Homann, P.S., Darbyshire, R.L., Morrissette, B.A., 2008. Intense forest wildfire sharply reduces mineral soil C and N: the first direct evidence. Canadian Journal of Forest Research 38, 2771–2783.
Bugmann, H., 2001. A review of forest gap models. Climate Change 51, 259–305.
Czimczik, C.I., Schmidt, M.W.I., Schulze, E.-D., 2005. Effects of increasing fire frequency on black carbon and organic matter in Podzols of Siberian Scots pine forests. European Journal of Soil Science 56, 417–428.
Davidson, E.A., Janssens, I.A., 2006. Temperature sensitivity of soil carbon decomposition and feedbacks to climate change. Nature 440, 165–173.
Djodjic, F., Borling, K., Bergstrom, L., 2004. Phosphorus leaching in relation to soil type and soil phosphorus content. Journal of Environment Quality 33, 678–684.
Fan, W., Randolph, J.C., Ehman, J.L., 1998. Regional estimation of nitrogen mineralization in forest ecosystems using geographic information systems. Ecological Applications 8, 734–747.
Fierer, N., Craine, J.M., Mclauchlan, K., Schimel, J.P., 2005. Litter quality and the temperature sensitivity of decomposition. Ecology 86, 320–326.
Gustafson, E.J., Shifley, S.R., Mladenoff, D.J., Nimerfro, K.K., He, H.S., 2000. Spatial simulation of forest succession and timber harvesting using LANDIS. Canadian Journal of Forest Research 30, 32–43.
Gustafson, E.J., Shvidenko, A.Z., Sturtevant, B.R., Scheller, R.M., 2010. Predicting global change effects on forest biomass and composition in south-central Siberia. Ecological Applications 20, 700–715.
Haeussler, S., Coates, D., 1986. Autecological characteristics of selected species that compete with conifers in British Columbia: a literature review. FRDA Report 001. Agriculture Canada, Ministry of State for Forestry and Mines, Pacific Forestry Center, Victoria, BC.
Harmon, M.E., Krankina, O.N., Sexton, J., 2000. Decomposition vectors: a new approach to estimating woody detritus decomposition dynamics. Canadian Journal of Forest Research 30, 76–84.
He, H.S., Mladenoff, D.J., 1999. Spatially explicit and stochastic simulation of forest–landscape fire disturbance and succession. Ecology 80, 81–99.
Johnson, D.W., Susfalk, R.B., Dahlgren, R.A., Klopatek, J.M., 1998. Fire is more important than water for nitrogen fluxes in semi-arid forests. Environmental Science and Policy 1, 79–86.
Johnson, D.W., Curtis, P.S., 2001. Effects of forest management on soil C and N storage: meta analysis. Forest Ecology and Management 140, 227–238.
Johnson, D.W., Murphy, J.D., Walker, R.F., Miller, W.W., 2007. Wildfire effects on forest carbon and nutrient budgets. Ecological Engineering 31, 183–192.
Keane, R.E., Ryan, K.C., Running, S.W., 1996. Simulating effects of fire in northern Rocky Mountain landscapes with the ecological process model FIRE-BGC. Tree Physiology 16, 319–331.
Laiho, R., Prescott, C.E., 1999. The contribution of coarse woody debris to carbon nitrogen, and phosphorus cycles in three Rocky Mountain coniferous forests. Canadian Journal of Forest Research 29, 1592–1603.
Laiho, R., Prescott, C.E., 2004. Decay and nutrient dynamics of coarse woody debris in northern coniferous forests: a synthesis. Canadian Journal of Forest Research 34, 763–777.
Landres, P.B., Morgan, P., Swanson, F.J., 1999. Overview of the use of natural variability in managing ecological systems. Ecological Applications 9, 1179–1188.
Lenhart, T., Eckhardt, K., Fohrer, N., Frede, H.-G., 2002. Comparison of two different approaches of sensitivity analysis. Physics and Chemistry of the Earth 27, 645–654.
Lutzow, M.V., Kogel-Knabner, I., Ekschmitt, K., Matzner, E., Guggenberger, G., Marschner, B., et al., 2006. Stabilization of organic matter in temperate soils: mechanisms and their relevance under different soil conditions—a review. European Journal of Soil Science 57, 426–445.
Manley, P.N., Fites-Kaufman, J.A., Barbour, M.G., Schlesinger, M.D., Rizzo, D.M., 2000. Biological integrity. GTR-PSW-175. USDA Forest Service, Albany, CA.
Manzoni, S., Trofymow, J.A., Jackson, R.B., Porporato, A., 2010. Stochiometric controls on carbon nitrogen, and phosphorus dynamics in decomposing litter. Ecological Monographs 80, 89–106.
Miller, R.O., 1998. High-temperature oxidation: dry ashing. In: Kalra, Y.P. (Ed.), Handbook of Reference Methods for Plant Analysis. CRC Press, Boca Raton, FL, pp. 53–56.
Mitchell, H.L., Chandler, R.F., 1939. The nitrogen nutrition and growth of certain deciduous trees of northeastern United States. Black Rock Forest Bulletin No. 11. Cornwall Press, Cornwall, NY.
Mladenoff, D.J., He, H.S., 1999. Design and behavior of LANDIS, and object-oriented model of forest landscape disturbance and succession. In: Mladenoff, D.J., Baker, W.L. (Eds.), Advances in Spatial Modeling of Forest Landscape Change: Approaches and Applications. Cambridge University Press, Cambridge, UK, pp. 163–185.
Moore, T.R., Trofymow, J.A., Prescott, C.E., Fyles, J., Titus, B.D., Group, C.W., 2006. Patterns of carbon, nitrogen, and phosphorus dynamics in decomposing foliar litter in Canadian forests. Ecosystems 9, 46–62.
Murphy, J.D., Johnson, D.W., Miller, W.W., Walker, R.F., Carroll, E.F., Blank, R.R., 2006. Wildfire effects on soil nutrients and leaching in the Lake Tahoe Basin watershed. Journal of Environment Quality 35, 479–489.
Nacify, C., Sala, A., Keeling, E.G., Graham, J., Deluca, T.H., 2010. Interactive effects of historical logging and fire exclusion on ponderosa pine forest structure in the Northern Rockies. Ecological Applications 20, 1851–1864.
Nave, L.E., Vance, E.D., Swanston, C.W., Curtis, P.S., 2011. Fire effects on temperate forest C and N storage. Ecological Applications 21, 1189–1201.
Niklas, K.J., Enquist, B.J., 2002. Canonical rules for plant organ biomass partitioning and annual allocation. American Journal of Botany 89, 812–819.

Noij, I.G.A.M., Janssen, B.H., Wesselink, L.G., Van Grinsven, J.J.M., 1993. Modeling Nutrient and Moisture Cycling in Tropical Forests. The Tropenbos Foundation, Wageningen, The Netherlands, 195 pp.
Ollinger, S.V., Smith, M.L., Martin, M.E., Hallett, R.A., Goodale, C.L., Aber, J.D., 2002. Regional variation in foliar chemistry and N cycling among forests of diverse history and composition. Ecology 83, 339–355.
Oreskes, N., Shrader-Frechette, K., Belitz, K., 1994. Verification, validation, and confirmation of numerical models in the earth sciences. Science 263, 641–646.
Parton, W.J., Schimel, D.S., Cole, C.V., Ojima, D.S., 1987. Analysis of factors controlling soil organic matter levels in Great Plains grasslands. Soil Science Society of America Journal 51, 1173–1179.
Parton, W.J., Stewart, J.W.B., Cole, C.V., 1988. Dynamics of C, N, P, and S in grassland soils: a model. Biogeochemistry 5, 109–131.
Pastor, J., Post, W.M., 1985. Development of a linked forest productivity–soil process model. ORNL/TM-9519. Oak Ridge National Laboratory, Oak Ridge, TN.
Pastor, J., Post, W.M., 1986. Influence of climate, soil moisture, and succession on forest carbon and nitrogen cycles. Biogeochemistry 2, 3–27.
Peng, C., Apps, M.J., 1999. Modelling the response of net primary productivity (NPP) of boreal forest ecosystems to changes in climate and fire disturbance regimes. Ecological Modelling 122, 175–193.
Pietikainen, J., Kiikkila, O., Fritze, H., 2000. Charcoal as a habitat for microbes and its effect on the microbial community of the underlying humus. Oikos 89, 231–242.
Prescott, C.E., Chappell, H.N., Vesterdal, L., 2000. Nitrogen turnover in forest floors of coastal Douglas-fir at sites differing in soil nitrogen capital. Ecology 81, 1878–1886.
Preston, C.M., Schmidt, M.W.I., 2006. Black (pyrogenic) carbon: a synthesis of current knowledge and uncertainties with special consideration of boreal regions. Biogeosciences 3, 397–420.
Raison, R.J., Khanna, P.K., Woods, P.V., 1985. Transfer of elements to the atmosphere during low-intensity prescribed fires in three Australian subalpine eucalypt forests. Canadian Journal of Forest Research 15, 657–664.
Rastetter, E.B., King, A.W., Cosby, B.J., Hornberger, G.M., O'neill, R.V., Hobbie, J.E., 1992. Aggregating fine-scale ecological knowledge to model coarser-scale attributes of ecosystems. Ecological Applications 2, 55–70.
Rastetter, E.B., 1996. Validating models of ecosystem response to global change. BioScience 46, 190–198.
Running, S.W., Hunt Jr., E.R., 1993. Generalization of a forest ecosystem process model for other ecosystems, BIOME-BGC, and an application for global-scale models. In: Ehleringer, J.R., Field, C.B. (Eds.), Scaling Physiological Processes: Leaf to Globe. Academic Press, San Diego, CA, pp. 141–157.
Scheller, R.M., Mladenoff, D.J., 2004. A forest growth and biomass module for a landscape simulation model LANDIS: design, validation, and application. Ecological Modelling 180, 211–229.
Scheller, R.M., Mladenoff, D.J., 2005. A spatially interactive simulation of climate change, harvesting, wind, and tree species migration and projected changes to forest composition and biomass in northern Wisconsin, USA. Global Change Biology 11, 307–321.
Scheller, R.M., Domingo, J.B., Sturtevant, B.R., Williams, J.S., Rudy, A., Gustafson, E.J., et al., 2007. Design, development, and application of LANDIS-II a spatial landscape simulation model with flexible temporal and spatial resolution. Ecological Modelling 201, 409–419.
Scheller, R.M., Hua, D., Bolstad, P.V., Birdsey, R.A., Mladenoff, D.J., 2011. The effects of forest harvest intensity in combination with wind disturbance on carbon dynamics in Lake States Mesic Forests. Ecological Modelling 222, 144–153.
Silver, W.L., Miya, R.K., 2001. Global patterns in root decomposition: comparisons of climate and litter quality effects. Oecologia 129, 407–419.
Verburg, P.S.J., Johnson, D.W., 2001. A spreadsheet-based biogeochemical model to simulate nutrient cycling processes in forest ecosystems. Ecological Modelling 141, 185–200.
Vitousek, P.M., Howarth, R.W., 1991. Nitrogen limitation on land and in the sea: how can it occur? Biogeochemistry 13, 87–115.
White, M.A., Thornton, P.E., Running, S.W., Nemani, R.R., 2000. Parameterization and sensitivity analysis of the BIOME-BGC terrestrial ecosystem model: net primary production controls. Earth Interactions 4, 1–85.
Wimberly, M.C., 2004. Fire and forest landscapes in the Georgia Piedmont: an assessment of spatial modeling assumptions. Ecological Modelling 180, 41–56.
Xu, C., He, H.S., Hu, Y., Chang, Y., Larsen, D.R., Li, X., et al., 2004. Assessing the effect of cell-level uncertainty on a forest landscape model simulation in northeastern China. Ecological Modelling 180, 57–72.
Xu, C., He, H.S., Hu, Y., Chang, Y., Li, X., Bu, R., 2005. Latin hypercube sampling and geostatistical modeling of spatial uncertainty in a spatially explicit forest landscape model simulation. Ecological Modelling 185, 255–269.